01 Apr 2008

Channel Estimation, Equalization and Phase Correction for Single Carrier Underwater Acoustic Communications

Jun Tao

Y. Rosa Zheng
Missouri University of Science and Technology, zhengyr@mst.edu

Chengshan Xiao
Missouri University of Science and Technology, xiaoc@mst.edu

Wen-Bin Yang

et. al. For a complete list of authors, see https://scholarsmine.mst.edu/ele_comeng_facwork/919

Recommended Citation

J. Tao et al., "Channel Estimation, Equalization and Phase Correction for Single Carrier Underwater Acoustic Communications," *Proceedings of MTS/IEEE Kobe Techno-Ocean OCEANS 2008*, Institute of Electrical and Electronics Engineers (IEEE), Apr 2008.
The definitive version is available at https://doi.org/10.1109/OCEANSKOBE.2008.4531083

Channel Estimation, Equalization and Phase Correction for Single Carrier Underwater Acoustic Communications

Jun Tao[†], Yahong Rosa Zheng[§], Chengshan Xiao[§], T. C. Yang[‡] and Wen-Bin Yang[‡]

[†]Dept. of Electrical & Computer Eng., University of Missouri-Columbia, MO 65211, USA

[§]Dept. of Electrical & Computer Eng., Missouri University of Science & Technology, Rolla, MO 65409, USA

[‡]Naval Research Laboratory, Washington, DC 20375, USA

***Abstract*— In this paper, we employ a time-domain channel estimation, equalization and phase correction scheme for single carrier single input multiple output (SIMO) underwater acoustic communications. In this scheme, Doppler shift, which is caused by relative motion between transducer (source) and hydrophones (receiver), is estimated and compensated in the received baseband signals. Then the channel is estimated using a small training block at the front of a transmitted data package, in which the data is artificially partitioned into consecutive data blocks. The estimated channel is utilized to equalize a block of received data, then the equalized data is processed by a group-wise phase correction before data detection. At the end of the detected data block, a small portion of the detected data is utilized to update channel estimation, and the re-estimated channel is employed for channel equalization for next data block. This block-wise channel estimation, equalization and phase correction process is repeated until the entire data package is processed. The receiver scheme is tested with experimental data measured at Saint Margaret's Bay, Nova Scotia, Canada, in May 2006. The results show that it can be applied not only to the scenario of fixed source to fixed receiver, but also to the moving source to fixed receiver case. The achievable uncoded bit error rate (BER) is on the order of 10^{-4} for moving-to-fixed transmissions, and on the order of 10^{-5} for fixed-to-fixed transmissions.**

I. Introduction

It is well known that shallow water horizontal communication channels are often hostile for high data rate underwater acoustic communications, which impose three major obstacles for coherent transceivers [2], [4], [5], [10], [11]. One is the excessive multipath delay spread in a medium range shallow water channel which usually causes the intersymbol interference (ISI) to extend over $20 - 300$ symbols at a data rate of $2 - 10$ kilosymbols per second. Another obstacle is the Doppler shift due to the source-receiver relative motion with high Doppler to carrier frequency ratios on the order of 10^{-3} to 10^{-4}, which causes compression or dilation on the received signals. As a result, time re-scaling is required on the received signal before channel estimation and equalization can be performed with satisfactory results. The third obstacle is the fast time-varying phase drift due to random medium of the underwater acoustic channels.

In the last fifteen years, various algorithms have been proposed for channel estimation and channel equalization in both time domain [3], [11], [16], [17] and frequency domain including single-carrier frequency domain equalization (SC-FDE) [18], and orthogonal frequency division modulation (OFDM) technique [13], [14], [15]. For the time-domain algorithm, it has been first demonstrated in [2] using joint decision feedback equalization (DFE) and phase synchronization of a phase-locked loop (PLL) or delay-locked loop (DLL). However, the system required careful placement and tuning of the equalizer taps and PLL/DLL coefficients which greatly affected its stability and robustness in different channel conditions. In [1], the single input multiple output (SIMO) multichannel system was considered for underwater acoustic communications. This work first introduced the optimum maximum likelihood sequence estimation (MLSE) receiver, then proposed a suboptimal structure which performed MMSE multichannel combining, fractionally spaced adaptive decision feedback equalization and carrier phase recovery jointly. The use of spatial diversity improved receiver performance with respect to noise and fading. However, the combination of adaptive DFE and PLL still made it difficult for the robust operation of the time-domain equalizer. Recently, reference [17] proposed an equalization and phase correction scheme, which addressed the convergence and robustness problem of conventional time-domain adaptive equalizers mentioned above. Specifically, this scheme separated the operations of equalization and phase correction. The developed phase estimation and compensation algorithm worked in a group-wise rather than a symbol-wise manner, and was robust to additive noise and channel condition. This scheme was employed to process experimental data of fixed source to fixed receiver with a transmission rate of 2 kilo-symbols per second.

In this paper, we employ the time-domain multichannel receiver structure of [17]. We present more details on the structure and algorithms. This structure with fine tuned parameters is employed to process experimental data of moving source to fixed receiver at a transmission data rate of 4 kilo-symbols per second. The results indicate that the scheme works effectively with uncoded bit error rate (BER) on the order of 10^{-4}. Naturally, it also works well in the scenario of fixed source and fixed receiver transmission, which is actually the special case of moving-to-fixed transmission when the relative velocity between source and receiver is close to zero. The

*Dr. W.-B. Yang is now with Information Technology Laboratory, National Institute of Standards and Technology, Gaithersburg, MD 20899.

978-1-4244-2126-8/08/$25.00 ©2008 IEEE

fixed-to-fixed transmission achieves an uncoded BER on the order of 10^{-5}, which is better than that of moving-to-fixed transmission. Without special specification, we call the fixed source to fixed receiver scenario as fixed transmission, and moving source to fixed receiver as moving transmission in the sequel.

II. System Model

For an underwater acoustic communication system employing single transducer source and M hydrophone receivers, the discrete-time baseband equivalent signal received at the m-th hydrophone is expressed as

$$r_m(k)=\sum_{l=0}^{L-1}\breve{h}_m(k,l)x(k-l)e^{j(2\pi f_{m,0}kT_s+2\pi\breve{f}_{m,k}kT_s+\theta_{m,0})}+n_m(k) \quad (1)$$

where k is the time index, T_s is the symbol interval, $x(k)$ is the transmitted data symbol or training symbol, $\{\breve{h}_m(k,l),\ 0\le l\le L-1\}$ are the fading coefficients of the frequency-selective, time-varying channel at time instant k with length L in terms of T_s, $f_{m,0}$ and $\breve{f}_{m,k}$ are the average Doppler shift (or CFO) and the instantaneous Doppler, respectively. The initial phase $\theta_{m,0}$ represents the phase error after coarse synchronization, and $n_m(k)$ is zero-mean additive white Gaussian noise (AWGN) with power σ^2. In many practical underwater acoustic systems [1], [2], [8], the fading channel coefficients $\breve{h}_m(k,l)$ usually changes much slower than the instantaneous phase $2\pi f_{0,k}kT_s+2\pi\breve{f}_{m,k}kT_s$, which ultimately makes it difficult for the channel equalization and coherent detection.

If the relative motion between the source and receiver is insignificant, then the average Doppler shift $f_{m,0}$ is close to zero, but the instantaneous Doppler $\breve{f}_{m,k}$ modeled as a zero-mean time-varying random variable still causes significant phase drift in the received symbols. If the average Doppler shift $f_{m,0}$ is significant, then it causes the transmitted signal $x(k)$ to be time-scaled (compressed or dilated) [4], [5], [6], [10]. In this case, Doppler estimation and compensation is necessary to achieve symbol synchronization before equalization takes place to cancel ISI. Specifically, denoting T_{tx} as the time duration of transmitted packet, and $T_{m,rx}$ as the time duration of received packet on the mth receiver, then the Doppler shift is estimated for the mth receiver as follows

$$\hat{f}_{m,0}=\left(1-\frac{T_{m,rx}}{T_{tx}}\right)\cdot f_c \quad (2)$$

where f_c is carrier frequency. Once the Doppler estimation $\hat{f}_{m,0}$ is obtained, $f_{m,0}$ can be compensated, and the re-sampling operation is performed on $r_m(k)$ in (1). The re-sampling frequency for the mth receiver is also determined by T_{tx} and $T_{m,rx}$, and is calculated as

$$f_{m,s}=\frac{T_{tx}}{T_{m,rx}}\cdot f_s \quad (3)$$

where $f_s=1/T_s$ is the original sampling frequency. Basically, the re-sampling can be implemented by interpolation methods, either using polyphase implementation or using linear interpolation. After Doppler compensation and re-sampling, the received samples in (1) can be rewritten as

$$y_m(k)=\sum_{l=0}^{L-1}h_m(k,l)x(k-l)e^{j(2\pi f_{m,k}kT_{m,s}+\theta_{m,0})}+v_m(k) \quad (4)$$

where $T_{m,s}=1/f_{m,s}$ is the re-sampling interval of the mth receiver, $y_m(k)$ denotes the re-sampled received signal, and $h_m(k,l)$, $f_{m,k}$ and $v_m(k)$ represent fading channel coefficient, instantaneous Doppler spread and additive noise after Doppler compensation and re-sampling, respectively. $v_m(k)$ is still zero-mean AWGN with variance σ^2.

III. Channel Estimation, Equalization and Phase Compensation

The block diagram of the employed receiver structure is depicted in Fig. 1, where the Doppler preprocessing has been detailed in last section, so we start from channel estimation in

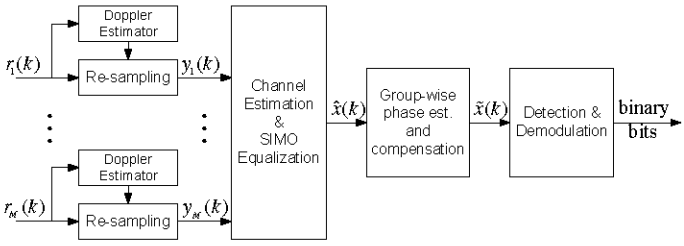

Fig. 1. New receiver structure (equalization and phase correction are decoupled).

this section. Channel estimation is obtained by using training symbols. When the time duration of the block of training symbols is much less than the channel coherence time, the fading channel coefficient $h_m(k,l)$ in (4) can be approximately treated as time-invariant, *i.e.*, $h_m(k,l)\approx h_m(l)$. Then equation (4) can be represented in matrix form as follows

$$\mathbf{y}_m=\mathbf{D}_m\mathbf{P}\mathbf{h}_m+\mathbf{v}_m \quad (5)$$

where

$$\mathbf{y}_m=[y_m(L-1),y_m(L),\cdots,y_m(N_p-1)]^T, \quad (6)$$

$$\mathbf{P}=\begin{bmatrix} p(L-1) & \cdots & p(1) & p(0) \\ p(L) & \cdots & p(2) & p(1) \\ \vdots & \ddots & \ddots & \vdots \\ p(N_p-1) & \cdots & p(N_p-L+1) & p(N_p-L) \end{bmatrix} \quad (7)$$

is the training matrix consisting of length-N_p training sequence $\{p(k),\ 0\le k\le N_p-1\}$, and

$$\begin{aligned}\mathbf{D}_m&=\mathrm{diag}\left\{\left[e^{j[2\pi f_{m,L-1}(L-1)T_{m,s}+\theta_{m,0}]},e^{j(2\pi f_{m,L}LT_{m,s}+\theta_{m,0})},\right.\right.\\&\qquad\left.\left.\cdots,e^{j[2\pi f_{m,N_p-1}(N_p-1)T_{m,s}+\theta_{m,0}]}\right]\right\}\\&\triangleq\mathrm{diag}\left\{\left[e^{j\phi_{m,0}},e^{j\phi_{m,1}},\cdots,e^{j\phi_{m,N_p-L}}\right]\right\} \quad (8)\end{aligned}$$

$$\mathbf{h}_m=[h_m(0),h_m(1),\cdots,h_m(L-1)]^T \quad (9)$$

978-1-4244-2126-8/08/$25.00 ©2008 IEEE

$$\mathbf{v}_m = [v_m(L-1), v_m(L), \cdots, v_m(N_p-1)]^T \quad (10)$$

are phase drift matrix, fading coefficient vector of the channel, and the noise vector, respectively. diag($\mathbf{a}$) denotes a diagonal matrix with row vector $\mathbf{a}$ on its diagonal, and T denotes vector transpose operation. In (5), $\mathbf{D}_m$ and $\mathbf{h}_m$ are separated by $\mathbf{P}$, and it's difficult to estimate the channel directly. To proceed, we rewrite $\mathbf{D}_m$ in (8) as

$$\mathbf{D}_m = e^{j\phi_{m,I}} \text{diag}\left\{\left[e^{j(\phi_{m,0}-\phi_{m,I})}, \cdots, e^{j(\phi_{m,N_p-L}-\phi_{m,I})}\right]\right\} \quad (11)$$

where the index I in $\phi_{m,I}$ is determined as $I = \lceil (N_p - L + 1)/2 \rceil$ with $\lceil x \rceil$ denoting the smallest integer larger than x. The instantaneous phase drift $\{\phi_{m,i} (0 \le i \le N_p - L)\}$ in (11) could be significant. However, the differential phase drift $\{\phi_{m,i} - \phi_{m,I} (0 \le i \le N_p - L)\}$ is insignificant over a short period of time. Then (11) is approximated as

$$\mathbf{D}_m \approx e^{j\phi_{m,I}} \mathbf{I} \quad (12)$$

with $\mathbf{I}$ being the $(N_p - L + 1) \times (N_p - L + 1)$ identity matrix. As a result, (5) can be rewritten as

$$\mathbf{y}_m = \mathbf{P}\left[e^{j\phi_{m,I}} \mathbf{h}_m\right] + \mathbf{v}_m \quad (13)$$

It has been shown in [7] that, at least $2L$–1 training symbols are required for accurate channel estimation for a multipath channel length of L. In our scheme, we choose $N_p > 2L-1$. The least square (LS) estimation of channel impulse response is obtained with (13) as

$$e^{j\phi_{m,I}} \hat{\mathbf{h}}_m \triangleq \hat{\mathbf{h}}_{c,m} = \mathbf{P}^{\dagger} \mathbf{y}_m \quad (14)$$

where † denotes pseudo inverse of matrix and

$$\hat{\mathbf{h}}_m = \left[\hat{h}_m(0), \hat{h}_m(1), \cdots, \hat{h}_m(L-1)\right]^T \quad (15)$$

$$\hat{\mathbf{h}}_{c,m} = \left[\hat{h}_{c,m}(0), \hat{h}_{c,m}(1), \cdots, \hat{h}_{c,m}(L-1)\right]^T \quad (16)$$

From (14), it's obvious that $\hat{h}_{c,m}(l) = e^{j\phi_{m,I}} \hat{h}_m(l),\ 0 \le l \le L-1$.

With the estimated channel coefficients, equalization can then be performed. The general form of the output of a feed forward SIMO linear equalizer is expressed as

$$\hat{x}(k) = \sum_{m=1}^{M} \sum_{q=-K_1}^{K_2} c_{m,q} y_m(k-q) \quad (17)$$

where K_1, K_2 are positive integers. $c_{m,q}$ denotes the qth equalizer coefficient on the m-th receiver, with q having the same range of $[-K_1, K_2]$ for all M receivers. In total, there are $M \times (K_1 + K_2 + 1)$ equalizer taps to be determined.

The SIMO equalizer coefficients $\{c_{m,q} (1 \le m \le M, -K_1 \le q \le K_2)\}$ designed with MMSE criteria is determined by the following equation [19]:

$$\begin{bmatrix} \boldsymbol{\Psi}_{1,1} & \boldsymbol{\Psi}_{1,2} & \cdots & \boldsymbol{\Psi}_{1,M} \\ \boldsymbol{\Psi}_{2,1} & \boldsymbol{\Psi}_{2,2} & \cdots & \boldsymbol{\Psi}_{2,M} \\ \vdots & \vdots & \vdots & \vdots \\ \boldsymbol{\Psi}_{M,1} & \boldsymbol{\Psi}_{M,2} & \cdots & \boldsymbol{\Psi}_{M,M} \end{bmatrix} \begin{bmatrix} \mathbf{C}_1 \\ \mathbf{C}_2 \\ \vdots \\ \mathbf{C}_M \end{bmatrix} = \begin{bmatrix} \mathbf{H}_1 \\ \mathbf{H}_2 \\ \vdots \\ \mathbf{H}_M \end{bmatrix} \quad (18)$$

where

$$\boldsymbol{\Psi}_{n,m} = \begin{bmatrix} \psi_{n,m,-K_1,-K_1} & \psi_{n,m,-K_1,-K_1+1} & \cdots & \psi_{n,m,-K_1,K_2} \\ \psi_{n,m,-K_1+1,-K_1} & \psi_{n,m,-K_1+1,-K_1+1} & \cdots & \psi_{n,m,-K_1+1,K_2} \\ \vdots & \vdots & \vdots & \vdots \\ \psi_{n,m,K_2,-K_1} & \psi_{n,m,K_2,-K_1+1} & \cdots & \psi_{n,m,K_2,K_2} \end{bmatrix}$$

$$\psi_{n,m,p,q} = \sum_{l=0}^{L-1} \hat{h}^*_{c,n}(l) \hat{h}_{c,m}(l+p-q) + \sigma^2 \delta_{n,m} \delta_{p,q}$$
$$(-K_1 \le p, q \le K_2; 1 \le n, m \le M)$$

$$\mathbf{C}_m = \left[c_{m,-K_1}, c_{m,-K_1+1}, \cdots, c_{m,K_2}\right]^T$$

$$\mathbf{H}_m = \left[\hat{h}^*_{c,m}(K_1), \hat{h}^*_{c,m}(K_1-1), \cdots, \hat{h}^*_{c,m}(-K_2)\right]^T$$

$*$ denotes conjugate operation, and $\delta_{n,m}, \delta_{p,q}$ are Kronecker delta functions.

Substituting (4) into (17), we get

$$\hat{x}(k) = \sum_{m=1}^{M} \sum_{q=-K_1}^{K_2} \sum_{l=0}^{L-1} c_{m,q} h_m(k-q,l) x(k-q-l) \times e^{j\left[2\pi f_{m,k-q}(k-q)T_{m,s} + \theta_{m,0}\right]} + \eta(k) \quad (19)$$

where $\eta(k)$ is the collection of additive noise $v_m(k)$ on all M receivers at the output of SIMO equalizer. When the span of q is not too large, the phase rotation caused by $f_{m,k-q}$ is insignificant, then (19) can be approximated as

$$\hat{x}(k) \doteq \sum_{m=1}^{M} e^{j(2\pi f_{m,k} k T_{m,s} + \theta_{m,0})} \times \left[\sum_{q=-K_1}^{K_2} \sum_{l=0}^{L-1} c_{m,q} h_m(k-q,l) x(k-q-l)\right] + \eta(k) \quad (20)$$

As we can see from (20), the double summation in the square bracket is the mth equalizer's output except for the phase outside of the square bracket. Therefore, we can define

$$\sum_{q=-K_1}^{K_2} \sum_{l=0}^{L-1} c_{m,q} h_m(k-q,l) x(k-q-l) \triangleq \alpha_m x(k) \quad (21)$$

where α_m denotes the scaling factor corresponding to the mth receiver, and it is usually a complex value closely relating to equalizer taps $\{c_{m,q}\}$. With (21), (20) is simplified as

$$\hat{x}(k) = \left[\sum_{m=1}^{M} \alpha_m e^{j\left(2\pi f_{m,k} k T_{m,s} + \theta_{m,0}\right)}\right] x(k) + \eta(k) = |\gamma_k| e^{j\angle\gamma_k} x(k) + \eta(k) \quad (22)$$

where $\gamma_k = \sum_{m=1}^{M} \alpha_m e^{j\left(2\pi f_{m,k} k T_{m,s} + \theta_{m,0}\right)}$.

Obviously, the M-receiver equalized symbol in (22), is the originally transmitted symbol after being scaled by a complex value γ_k on one side and corrupted by additive noise on the other side. When signal-to-noise ratio (SNR) is high, the effect of noise is insignificant. The complex scaling factor, which is actually the diversity combining gain of SIMO equalizer,

978-1-4244-2126-8/08/$25.00 ©2008 IEEE

however, introduces undesirable phase rotation $\angle\gamma_k$ into the transmitted symbol irrespective of the gain it brings. The phase rotation is especially hostile for modulation schemes like phase shift keying (PSK) and quadrature amplitude modulation (QAM), so it must be compensated after the equalization and before detection. The phase rotation $\angle\gamma_{m,k} = 2\pi f_{m,k} kT_{m,s} + \theta_{m,0} + \angle\alpha_m$ of the mth receiver indicates that it's jointly caused by instantaneous Doppler spread $f_{m,k}$, initial timing-error phase offset $\theta_{m,0}$, and the corresponding scaling factor α_m. The combined phase rotation of all M receivers is even more complicated, which makes phase correction a challenging task.

It is noted here that the separation of channel equalization and phase correction have been previously proposed using passive phase conjugation techniques [9], [10], and via decision-feedback phase-locked loop [12] for time-reversal underwater communications. However, the phase estimation we adopted from [17], is different from these aforementioned techniques. It utilizes a few training symbols and the equalized data to perform group-wise phase estimation and compensation, therefore, it has the advantages of insensitivity to noise perturbation, channel conditions and residual Doppler. The details can be found in [17], [18], and are omitted here for brevity.

IV. Experimental Results

Several experiments were conducted at Saint Margaret's Bay, Nova Scotia, Canada, in May 2006. Eight hydrophones were arranged unequally spaced over 1.86 meters on a vertical linear array. The array was deployed in water of 30 m depth. For moving transmission, the transducer was deployed in water at 21 m depth and towed at speed of about 4 knots, and the communication range was ranging from 1 km to 3 km. For fixed transmission, the transducer was suspended in water at 21 m depth and 44 m above the bottom, and the source-receiver range was 3.06 km. The QPSK signals with a bandwidth of 4 kHz were transmitted on a carrier frequency of 17 kHz. The transmitted signals were partitioned into packets. The signal structure of one packet is shown in Fig. 2. As can be seen that each packet is preceded by a linear frequency modulation (LFM) signal, which we called LFMB. The LFMB is followed by a gap, plus a probe signal followed by another gap. Then, it is the data package consisting of 40397 symbols. At the front of the data package, a small block of training symbols is used for initial channel estimation. The block size N_p is selected according to the channel length L, as mentioned before. The whole packet was ended by another LFM signal named as LFME, which was separated from the data package with a gap. During transmission, gaps that were sufficiently long were introduced among packets for avoiding inter packet interference.

For moving transmission, the received data packet duration was measured by correlating it with LFMB and LFME chirp signals attributing to their large bandwidth-time product. At the same time, coarse synchronization was achieved with LFMB correlation. With the estimated duration of received data packet, average Doppler shift was calculated and then

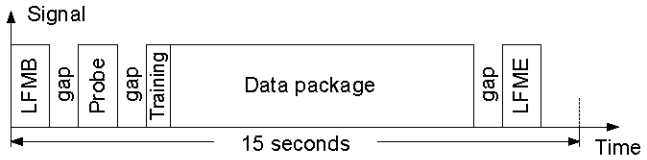

Fig. 2. Packet structure.

compensated in the received signal. For fixed transmission, Doppler shift estimation was not required, and the coarse synchronization was carried out by the probe signal, which was a m-sequence of 1023 bits.

In Table 1, the results of Doppler shift estimation are presented for 4 packets in the moving transmission. For each packet, Doppler shift is estimated individually on each receiver corresponding to one single transmission channel. Obviously, the estimated Doppler shifts are non-negligible compared to carrier frequency $f_c = 17$kHz. We also observe that, for a specific packet, the differences in Doppler shift estimations across channels are very small.

Table 1: Doppler shift estimation (Hz)

Packet	1	2	3	4
Channel 1	15.98	15.71	12.44	10.80
Channel 2	15.98	15.71	12.44	10.80
Channel 3	15.98	15.71	12.44	10.80
Channel 4	15.98	15.71	12.44	10.80
Channel 5	15.98	15.71	12.44	10.80
Channel 6	16.16	15.71	12.44	10.89
Channel 7	15.98	15.71	12.44	10.80
Channel 8	15.98	15.71	12.44	10.80

The channel length L was also estimated by LFMB. This was achieved by detecting the span of the main ridge, where correlation peak was centered, of the correlation output at the coarse synchronization stage. To demonstrate, we plot the range of LFMB correlation output centered at the peak in Fig. 3. From the figure, we find that most of the correlation energy is concentrated within 5ms which corresponding to a multipath length of $L = 20$ in terms of symbol period $T_s = 0.25ms$. Similar process was applied to fixed transmission, where the channel length was estimated to be $L = 60$ taps, which was larger than the moving source case due to longer communication range.

Based on the estimated channel length of $L = 20$, we used $N_p = 40$ symbols at the front of the data package for initial channel estimation. The rest of data in the package was artificially partitioned into consecutive blocks for block-wise channel estimation and equalization purpose as demonstrated in Fig. 4. The initially estimated channel impulse responses of the eight channels were then employed to equalize the first block of the data message in the packet. The block size was selected such that the corresponding time duration not exceeding the channel coherence time. In our processing, we chose a block size of $N_{blk} = 1600$, which was 0.4 seconds of time duration, and $K = 200$. The equalized data in the

978-1-4244-2126-8/08/$25.00 ©2008 IEEE

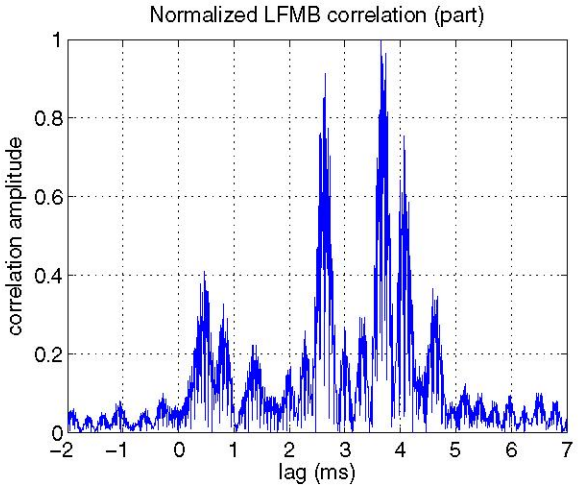

Fig. 3. Main ridge of LFMB correlation.

first block was then used to estimate and correct the time-varying phase drift with the group-wise phase estimation and compensation algorithm. A group size of $N_s = 40$ was selected for the group-size phase drift estimation algorithm. In total, there were $N_g = 40$ groups in one block. The equalized and phase-corrected data were then demodulated to obtain the binary information bits. When the detection for the first block was finished, the channel was re-estimated with the detected data symbols, and the updated channel coefficients was then used for processing the next block. Similar procedure continued until the whole data package was finished.

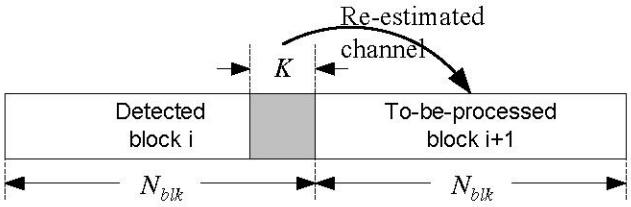

Fig. 4. Channel re-estimation (the last K detected symbols in previous block are used to re-estimate channel for the next block).

The scatter plots in Figs. 5, 6 and 7 are the original received baseband signals, the equalized signals, and the phase-corrected QPSK signals, respectively, with the moving transmission. Fig. 6 clearly shows that the suggested SIMO equalizer works well with respect to the symbol amplitude, while fails with respect to symbol phase. This observation matches the theoretical analysis and explanation given in last section. In Fig. 7, it's obvious that most of the symbols can be properly classified except a few. So the group-wise phase estimation and compensation algorithm works effectively with the moving transmission. The fixed transmission basically has less error symbols after demodulation compared to moving transmission.

The average uncoded BER of moving transmission with different numbers of channel diversity is listed in Table 2. Except the 40 training symbols used for initial channel estimation, there are in total 40357 out of 40397 available symbols carrying 80714 information bits. The results are averaged with 4 packets. Clearly, BER decreases when the number of channels used for diversity increases. When 8 channels are used, an uncoded BER on the order of 10^{-4} is achieved. We also list the average uncoded BER of fixed transmission in Table 3. In this case, four packets with each having 80554 available information bits, are used for average. Compared with moving transmission, the fixed transmission has better BER performance, which is on the order of 10^{-5} with 8 channels diversity. This observation is reasonable since the fixed transmission is not affected by Doppler shift.

Table 2: Average uncoded BER of moving transmission

number of channels	number of message bits	mean number of bit errors	mean bit error rate
1	80714	31611	0.3916
2	80714	30293	0.3753
3	80714	8728	0.1081
4	80714	1036	1.28×10^{-2}
5	80714	313	3.88×10^{-3}
6	80714	243	3.01×10^{-3}
7	80714	83	1.03×10^{-3}
8	80714	31	3.84×10^{-4}

Table 3: Average uncoded BER of fixed transmission

number of channels	number of message bits	mean number of bit errors	mean bit error rate
1	80554	32114	0.3987
2	80554	28545	0.3544
3	80554	3051	3.79×10^{-2}
4	80554	872	1.08×10^{-2}
5	80554	173	2.15×10^{-3}
6	80554	140	1.74×10^{-3}
7	80554	25	3.10×10^{-4}
8	80554	6	7.45×10^{-5}

V. Conclusion

A time-domain channel estimation, equalization and phase correction scheme has been adopted for single carrier SIMO underwater acoustic communication scenarios. The receiver scheme was tested by experimental data collected at Saint Margaret's Bay, Nova Scotia, Canada, in May 2006. The results has shown that the receiver scheme worked effectively for moving source to fixed receiver with uncoded BER on the order of 10^{-4} when 8 hydrophones were employed and communication range was about 1-3 km for QPSK modulation at carrier frequency of 17 kHz and symbol rate of 4 kilo-symbol per second. The receiver achieved an uncoded BER performance on the order of 10^{-5} for fixed-fixed transmission at communication range of 3.06 km, while the rest parameters were kept unchanged.

978-1-4244-2126-8/08/$25.00 ©2008 IEEE

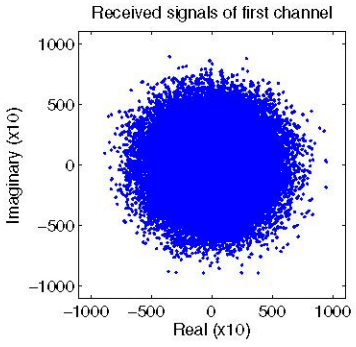

Fig. 5. Scatter plot of received signals of the first channel.

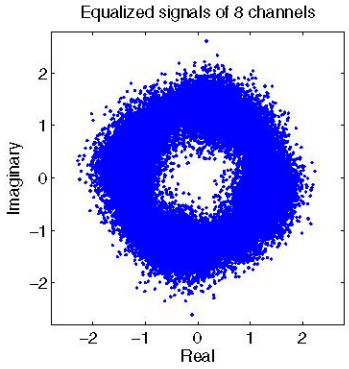

Fig. 6. Scatter plot of equalized QPSK signals using 8 channels.

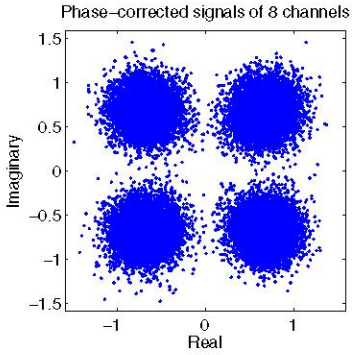

Fig. 7. Scatter plot of equalized and phase-corrected QPSK signals using 8 channels.

ACKNOWLEDGMENTS

This work of Y. R. Zheng and C. Xiao was supported in part by the Office of Naval Research under Grant N00014-07-1-0219 and the National Science Foundation under Grant CCF-0514770. The work of T. C. Yang and W.-B. Yang was supported by the Office of Naval Research.

REFERENCES

[1] M. Stojanovic, J. Catipovic, and J. Proakis, "Adaptive multichannel combining and equalziation for underwater acoustic communications," *J. Acoust. Soc. Amer.*, vol.94, pp.1621-1632, Jan. 1993.

[2] M. Stojanovic, J. Catipovic, and J. Proakis, "Phase-coherent digital communicaitons for underwater acoustic channels," *IEEE J. Ocean. Eng.*, vol.19, pp.100-111, Jan. 1994.

[3] M. Stojanovic, L. Freitag, and M. Johnson, "Channel-esitmation-based adaptive equalization of underwaner acoustic signals," in *Proc. MTS/IEEE OCEANS'99*, vol.2, 985-990, 1999.

[4] B. S. Sharif, J. Neasham, O. R. Hinton, and A. E. Adams, "A computationally efficient Doppler compensation system for underwater acoustic communications," *IEEE J. Ocean. Eng.*, vol.25, pp.52-61, Jan. 2000.

[5] T. H. Eggen, A. B. Baggeroer, and J. C. Preisig, "Communication over Doppler spread channels – Part I: channel and receiver presentation," *IEEE J. Ocean. Eng.*, vol.25, pp.62-71, Jan. 2000.

[6] T. C. Yang, "Underwater telemetry method using Doppler compensation," U.S. Patent No. 6,512,720, Jan. 2003.

[7] J. Wu, C. Xiao, and J. C. Olivier, "Time-varying and frequency-selective channel estimation with unequally spaced pilot symbols," *Int. J. Wireless Information Networks*, vol.11, no.2, pp.93-104, April 2004.

[8] T. C. Yang, "Differences between passive-phase conjugation and decision-feedback equalizer for underwater acoustic communications," *IEEE J. Ocean. Eng.*, vol.29, pp.472-487, April 2004.

[9] J. A. Flynn, J. A. Ritcey, D. Rouseff, and W. L. J. Fox, "Multichannel equalization by decision-directed passive phase conjugation: experimental results," *IEEE J. Ocean. Eng.*, vol.29, pp.824-836, July 2004.

[10] T. C. Yang, "Correlation-based decision-feedback equalizer for underwater acoustic communications," *IEEE J. Ocean. Eng.*, vol.30, pp.865-880, Oct. 2005.

[11] J. C. Preisig, "Performance analysis of adaptive equalization for coherent acoustic commuications in the time-varying ocean environment," *J. Acoust. Soc. Am*, vol.118, pp.263-278, 2005.

[12] H. C. Song, W. S. Hodgkiss, W. A. Kuperman, M. Stevenson, and T. Akal, "Improvement of time-reversal communications using adaptive channel equalizers," *IEEE J. Ocean. Eng.*, vol.31, pp.487-496, April 2006.

[13] M. Stojanovic, "Low complexity OFDM detector for underwater acoustic channels," in *Proc. Oceans'06*, 2006.

[14] B. Li, S. Zhou, M. Stojanovic, and L. Freitag, "Pilot-tone based ZP-OFDM demodulation for an underwater acoustic channel," in *Proc. Oceans'06*, 2006.

[15] B. Li, S. Zhou, M. Stojanovic, L. Freitag, and P. Willett, "Non-uniform Doppler compensation for zero-padded OFDM over fast-varying underwater acoustic channels," in *Proc. Oceans'07*, Aberdeen, Scotland, June 2007

[16] P. Gendron, "High frequency coherent acoustic commuications for the networked automomous littoral surveillance system," in *Proc. IEEE/OES OCEANS'07*, Aberden, Scotland, June 2007.

[17] Y. R. Zheng, "Channel estimation and phase-correction for robust underwater acoustic communications," in *Proc. IEEE Military Communications Conf. (MilCom07)*, Orlando, Oct. 2007.

[18] Y. R. Zheng, C. Xiao, T. C. Yang, and W. B. Yang, "Frequency-Domain Channel Estimation and Equalization for Single Carrier Underwater Acoustic Communications," in *Proc. Oceans'07*, Vancouver, Canada, 2007.

[19] J. G. Proakis and M. Salehi, *Digital Communication*, 5th Ed. Upper Saddle River, NJ: McGraw-Hill, 2008